1-1-2015

EPR Methods for Biological Cu(II): L-Band CW and NARS

Brian Bennett
Marquette University, brian.bennett@marquette.edu

Jason M. Kowalski
Medical College of Wisconsin

Accepted version. *Methods in Enzymology*, Vol. 563, (2015): 341-361. DOI.

EPR Methods for Biological Cu(II): L-Band CW and NARS

Brian Bennett

Physics Department, Marquette University, Milwaukee, WI

Jason M. Kowalski

Department of Chemistry, University of Wisconsin-Parkside, Kenosha, WI

Abstract: Copper has many roles in biology that involve the change of coordination sphere and/or oxidation state of the copper ion. Consequently, the study of copper in heterogeneous environments is an important area in biophysics. EPR is a primary technique for the investigation of paramagnetic copper, which is usually the isolated Cu(II) ion, but sometimes as Cu(II) in different oxidation states of multitransition ion clusters. The gross geometry of the coordination environment of Cu(II) can often be determined from a simple inspection of the EPR spectrum, recorded in the traditional X-band frequency range (9–10 GHz). Identification and quantitation of the coordinating ligand atoms, however, is not so straightforward. In particular, analysis of the superhyperfine structure on the EPR spectrum, to determine the number of coordinated nitrogen atoms, is fraught with difficulty at X-band, despite the observation that the overwhelming number of EPR studies of Cu(II) in the literature have been carried out at X-band. Greater reliability has been demonstrated at S-band (3–4 GHz), using the low-field parallel (g_z) features. However, analysis relies on clear identification of the outermost

Methods in Enzymology, Vol 563 (2015): pg. 341-361. DOI.

superhyperfine line, which has the lowest intensity of all the spectral features. Computer simulations have subsequently indicated that the much more intense perpendicular region of the spectrum can be reliably interpreted at L-band (2 GHz). The present work describes the development of L-band EPR of Cu(II) into a routine method that is applicable to biological samples.

Keywords: Copper; Electron paramagnetic/spin resonance; L-band; Nitrogen; Coordination

1. Background and Introduction

Copper is an element that is essential to life, but is also involved in many diseases and medical conditions (Tisato, Marzano, Porchia, Pellei, & Santini, 2009). Copper can activate or inhibit enzymes and transporters, promote or suppress redox processes in proteins, promote or inhibit aggregation or fibrillation of proteins, and modulate gene expression (Linder and Hazegh-Azam, 1996, Malmstrøm and Leckner, 1998, Perrone et al., 2009, Puig and Thiele, 2002 and Valentine and Gralla, 2002). Roles of copper in enzymes include electron transfer, oxygen activation, oxygen reduction, and denitrification (Solomon et al., 2014). The interaction of copper with proteins is suspected to be involved in prion diseases (prion protein, "PrP"; Leach et al., 2006, Millhauser, 2007, Nadal et al., 2007, Roucou and LeBlanc, 2005, Varela-Nallar et al., 2006, Varela-Nallar, et al., 2006, Wong et al., 2004 and Zidar et al., 2008), Alzheimer's disease (amyloid precursor protein A; Barnham and Bush, 2008, Bayer et al., 2006, Bush, 2008, Bush and Tanzi, 2008, Crouch et al., 2007, Crouch et al., 2009, Drew et al., 2009, Huang et al., 1999 and Maynard et al., 2005), and Parkinson's disease (α-synuclein; Brown, 2009 and Wright and Brown, 2008). Cu/Zn superoxide dismutase is a key player in amyotrophic lateral sclerosis (ALS) (Vucic & Kiernan, 2009) and interactions of Cu with P-type copper-transporting ATPases are important in Menke's and Wilsons's diseases (de Bie et al., 2007, La Fontaine and Mercer, 2007 and Pfeiffer, 2007), multidrug resistance and drug transport (Furukawa, Komatsu, Ikeda, Tsujikawa, & Akiyama, 2008), cancer, and anticancer drug resistance (Kuo et al., 2007 and Zhang et al., 2009). The architecture of serum amyloid A assemblies is Cu dependent (Wang & Colon, 2007) and Cu may play a role in metabolic syndrome (Park, Shin, Kim, Hong, & Cho, 2010). Formation and stabilization by copper of spherical aggregates of

ubiquitin are characteristics of the progression of Alzheimer's, Parkinson's, and ALS (Arnesano et al., 2009).

Two recent detailed reviews are highly recommended to the reader with a keen interest in the biophysical study of copper in biological systems (Antholine et al., 2011 and Solomon et al., 2014). An extensive review of copper in biologically active sites, by Solomon and coworkers (from here on simply referred to as "the Solomon review"); Solomon et al. (2014) described the electronic structure, electronic structure calculation methods, and relevant spectroscopies (X-ray-based XAS, XES, and XMCD; optical and magneto-optical; and EPR, ENDOR, and electron spin-echo envelope-modulation (ESEEM)), pertaining to Cu(I), Cu(II), and multicopper sites in copper-containing enzymes. In the latter, consideration was primarily afforded to copper centers in enzymes with roles in electron transfer, oxygen activation, oxygen reduction, and denitrification. Notably absent from the Solomon review were (i) a discussion of multifrequency, particularly low-frequency EPR, and (ii) descriptions of the copper environments in copper chaperones, and in proteins that bind copper and that are associated with neurological diseases, including prions, amyloids, and synucleins. The other, in many ways complementary, review described multifrequency EPR of copper in various coordination environments (this review will be referred to as the "ABH review" after the initials of the authors, Antholine, Bennett, and Hanson) (Antholine et al., 2011). An introduction to the principles and benefits of multifrequency EPR was first presented with reference to a number of different spin systems, including Cu(II), Mo(V), and Fe(III) and other high-spin systems. There was an emphasis on computer simulation as both a tool for determining spin-Hamiltonian parameters and for learning more fundamentally about the influence of microwave frequency and applied magnetic field on observed transitions. The application of multifrequency EPR, and particularly low-frequency EPR, to Cu(II) was then developed, and the reader is referred to this section of the ABH review in particular as a complement to the present treatment. The ABH review concluded with a survey of experimental studies involving S-(3.4 GHz), C-(4.5 GHz), X-(9 GHz), and Q-band (35 GHz) EPR. Finally, it would be remiss of the present authors not to refer the reader to the section on Cu(II), and additionally to the important appendices K & L, in Pilbrow's seminal work (Pilbrow, 1990), that provides an informative introduction to this field.

Methods in Enzymology, Vol 563 (2015): pg. 341-361. DOI.

Since the publication of the ABH review, the most exciting developments that have occurred in the domain of low-frequency EPR of Cu(II) are (i) the development of L-band (2 GHz) as an almost routine technique for the study of Cu(II) in biological material at reasonable amounts (≥ 50–100 nmol) and (ii) the development of nonadiabatic rapid sweep (NARS) EPR at 2 GHz and its subsequent application to Cu(II) (Hyde et al., 2013, Hyde et al., 2009, Kittell et al., 2011, Kittell et al., 2012, Kittell and Hyde, 2015 and Kowalski and Bennett, 2011).

2. Information from EPR of Cu(II)

EPR spectroscopy has long been used to probe Cu(II) in biological environments, almost since the initial reports in 1945 and 1946 by Zavoisky of the paramagnetic resonance of Cu(II) salts (Kochelaev & Yablokov, 1995). The reasons for performing EPR studies of Cu(II) in biological systems are manifold and include (i) identification of copper; (ii) characterization of geometry of the copper ion(s); (iii) characterization of the ligand sphere; (iv) determination of the number, oxidation states and spin-couplings of copper, and/or other transition ions in multi-ion centers or proteins; and (v) spectrokinetic studies of copper active sites or of copper transport and insertion (Antholine et al., 2011, Bennett and Hill, 2011 and Solomon et al., 2014). In the case of (i) and (ii), an understanding of the "anatomy" of a Cu(II) EPR signal at a particular frequency is almost always sufficient to unambiguously identify Cu(II) and determine its gross geometry, as the g-values and associated $I = 3/2$ hyperfine couplings are well documented and understood from a theoretical perspective (Pilbrow, 1990 and Solomon et al., 2014). Briefly, for tetragonal and related square-planar-based geometries, an essentially axial spectrum is expected with $g_{||} > g_{\perp} > 2$. A highly axial hyperfine interaction with the $I = 3/2$ ^{63}Cu or ^{65}Cu nucleus is manifested as a splitting of the $g_{||}$ resonance into four lines, of which either three or four are typically resolved at X-band, depending on the coordination and its effect on the spin-Hamiltonian parameters (Peisach & Blumberg, 1974); typical spectra are shown in Fig. 1. The spectra are a consequence of the nominally d$x^2 - y^2$ ground state paramagnetic orbital (better described as d$x^2 - y^2$/dxy for lower than ideal symmetry). Severe distortion of tetragonal geometry may, however,

Methods in Enzymology, Vol 563 (2015): pg. 341-361. DOI.

introduce mixing of the dz^2 orbital into the paramagnetic orbital. This results in a now rhombic **g** tensor, with $g_z > g_y > g_x \cong 2$, and $A_z > A_x \gg A_z$, where a four-line pattern is typically only resolved in the *z* and *x* orientations (lowest- and highest-field electronic Zeeman resonances, respectively) at X-band. For geometries with a formal dz^2 paramagnetic ground state, most notably trigonal bipyramidal in biological systems, then $g_\perp > g_{||} = 2.0$. It is often, then, a reasonably straightforward exercise to determine the gross geometry of a Cu(II) center from the EPR spectrum at X-band. Characterization of copper in multi-ion clusters is more challenging and, apart from the so-called $[Cu^{1.5}Cu^{1.5}]$ $S = 1/2$ centers, the information available and the optimum means by which to extract it is largely a function of the interspin interactions and consequent effective zero-field splittings (Antholine et al., 2011 and Solomon et al., 2014).

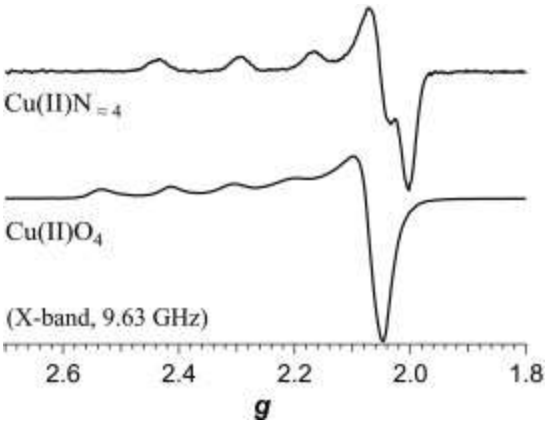

Figure 1. X-band EPR spectra of copper coordinated to α-synuclein (top) and in aqueous solution (bottom).

The most desirable, but often the most challenging, information from EPR is a description of the ligand coordination sphere, particularly in systems that are not amenable to high-resolution structural techniques. In a recent spectrokinetic study, for example, EPR was used to track the change in the equatorial coordination of tetragonal Cu(II) during binding by the *Bacillus subtilis* chaperone involved in Cu site assembly in cytochrome oxidase (BsSCO) from CuO_4 in free solution (as $[Cu(H_2O)_6]^{2+}$), via a transient (10 to > 140 ms) CuO_2N_2 state, to the final previously characterized and stable CuN_2S_2 state (Bennett & Hill, 2011). Identification of Cu(II) binding to a quasi-stable preliminary binding site explained how Cu(II) could come to be bound in the destination dithiolate binding site without risk of promoting

Methods in Enzymology, Vol 563 (2015): pg. 341-361. DOI.

autoxidation of the sulfhydryls. However, that study also highlighted the challenges of determining the ligand sphere from EPR, particularly at X-band and relied solely on the Peisach–Blumberg relationships to characterize the CuO_4 and CuO_2N_2 species (additional support for two coordinated nitrogen atoms in the equilibrium bound CuN_2S_2 species was provided by simultaneous computer simulation of the particularly well-resolved X- and Q-band EPR spectra). In their approach, Peisach and Blumberg identified regions on a plot of $A_{||}$ versus $g_{||}$ that correspond to particular combinations of equatorially coordinated sulfur, nitrogen, and oxygen; 2N2S ($=Cu^{II}N_2S_2$), 2N2O, 4S, 4N, and 4O (see Fig. 2) (Peisach & Blumberg, 1974). The correlations are imprecise (imagine, for example, how CuS_2NO, CuO_2S_2, or $CuSN_2O$ would present) and the 2N2O and 4N regions not only overlap extensively themselves but, over one small area, mutually overlap with 4O! Nevertheless, in many cases, the correlations provide some valuable information and have the advantage that the coordination of sulfur or oxygen can be detected in the absence of any reliance on electron–nuclear superhyperfine interaction. The ability of DFT calculations to provide structural models for copper coordination environments based on spin-Hamiltonian parameters is becoming increasingly reliable (Comba et al., 2008), although extraction of those parameters from traditional X-band EPR spectra is not as straightforward as is sometimes supposed (Kowalski & Bennett, 2011). Nitrogen, of course, carries a nuclear spin, $I = 1$, that provides a three-line multiplet where resolved, so the number of coordinated nitrogens and their superhyperfine coupling constants along the principal electronic Zeeman axes $g_{xx, yy, zz}$ are in principle derivable from the EPR spectrum, though this is often not realized in practice due to phenomenological factors that include strain-broadened line widths, overlap of $A(^{14}N)$ with $A_{\perp}(^{63/65}Cu)$, spectral broadening due to the two isotopes of copper present, and overlap of the principal electronic Zeeman resonances with the "overshoot" or "angular anomaly" line(s) (Ovchinnikov & Konstaninov, 1978). As was highlighted in a recent study by the present authors, the resolved ^{14}N superhyperfine and $^{63/65}Cu$ hyperfine patterns on the perpendicular electronic Zeeman turning point ($g_{\perp}$) are often the only highly resolved features of the spectrum at X-band but lie in a deceptively complex region of the spectrum and do not reliably distinguish between CuN_3 and CuN_4 equatorial coordination (Kowalski & Bennett, 2011). Finally,

Methods in Enzymology, Vol 563 (2015): pg. 341-361. DOI.

copper also exhibits non-negligible quadrupolar interactions, **I·P·I**, which in principle can provide information on geometry and symmetry that can, in turn, inform on the ligand sphere. However, quadrupolar interactions can be very difficult to obtain from EPR (Abrakhmanov and Ivanova, 1978, Belford and Duan, 1978 and White and Belford, 1976).

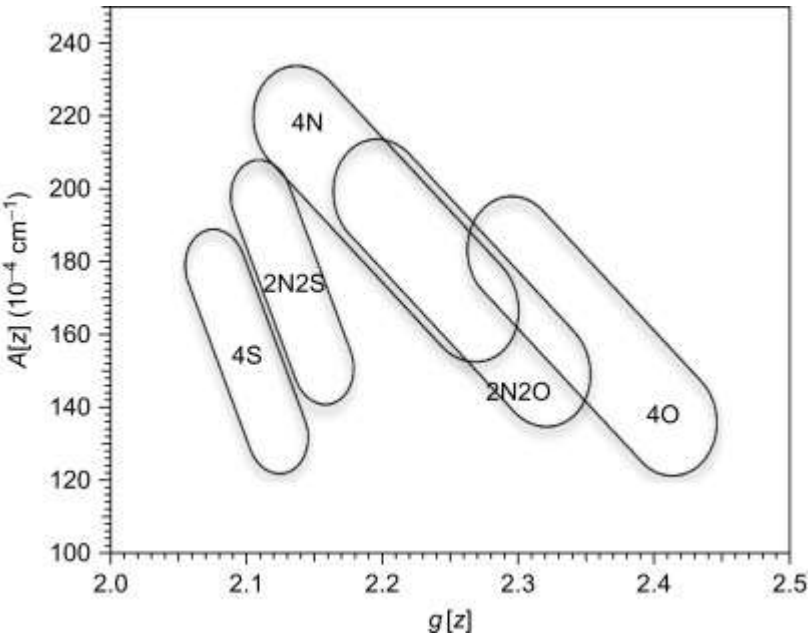

Figure 2. $A_{||}$ versus $g_{||}$ for various copper coordination spheres. Data adapted from Peisach and Blumberg (1974).

3. Strain Broadening, Isotope Broadening, and the Overshoot Line

Strain broadening is a term used to denote the frequency-dependent broadening of the line width, Δ, where, here, $\Delta = \sqrt{[\Delta^2_{\text{intrinsic}} + (m_I\sigma A)^2 + [(h\nu/g^2\beta_e)\sigma g]^2 - 2\varepsilon m_I(h\nu/g^2\beta_e)\sigma g\sigma A]}$ for the m_I manifolds of the $I = 3/2$ hyperfine-split resonances of a tetragonal system (Froncisz et al., 1980, Froncisz et al., 1979 and Hyde and Froncisz, 1982). In this expression, σg and σA represent distributions ("strains") in the principal values of g and A due to microheterogeneity of the electronic structures of the Cu(II) ions in the sample. This may be due, for example, to the immobilization of low-lying conformational/vibrational substates upon freezing of a solution in liquid nitrogen. Model strain-dependent line widths (Hyde, Antholine, Froncisz, & Basosi, 1986) for m_I manifolds of the $g_{||}$ resonance of

Methods in Enzymology, Vol 563 (2015): pg. 341-361. DOI.

Cu(II) as a function of microwave frequency are shown graphically in Fig. 3. At frequencies approaching X-band, and at all frequencies above, it can be seen from Fig. 3 that the line width of each resonance increases linearly and rapidly with frequency, as the *g*-strain-dependent field envelope of the resonant line, $\Delta B_g \propto \nu/\sigma g$ (i.e., $\propto \nu$), whereas its hyperfine-dependent analog ΔB_A is field-(frequency) independent and rapidly becomes insignificant at higher frequencies. At lower frequencies, however, where $\Delta B_g \cong |\Delta B_A|$, then, for two of the four $I = 3/2$ lines, the term $-2\varepsilon m_I(h\nu/g^2\beta_e)\sigma g\sigma A$ must adopt a negative value. Depending on the values of the strains themselves and the *g*-strain–*A*-strain coupling, ε, the *g*- and *A*-strains consequently more-or-less cancel each other in a frequency-dependent manner, and a frequency will exist for each of the two lines at which optimal *strain narrowing* will be observed. This phenomenon can be exploited using multifrequency EPR to optimize the extraction of the number of equatorially coordinated nitrogen atoms, a goal often of value, e.g., in determining the order of binding, or partition of, copper in multisite proteins (Chattopadhyay et al., 2005, Hyde et al., 2009 and Kowalski and Bennett, 2011). (Note that while for some systems, e.g., thiolate-coordinated Cu(II) or Cu(II)-substituted heme proteins, significant strain narrowing of the lowest-field $m_I = +3/2$ manifold may be observed between 3.5 and 9 GHz (Hyde et al., 1986 and Pasenkiewicz-Gierula, Antholine, et al., 1987) *g*-strain broadening precludes superhyperfine resolution of this manifold for most biological Cu(II) species.)

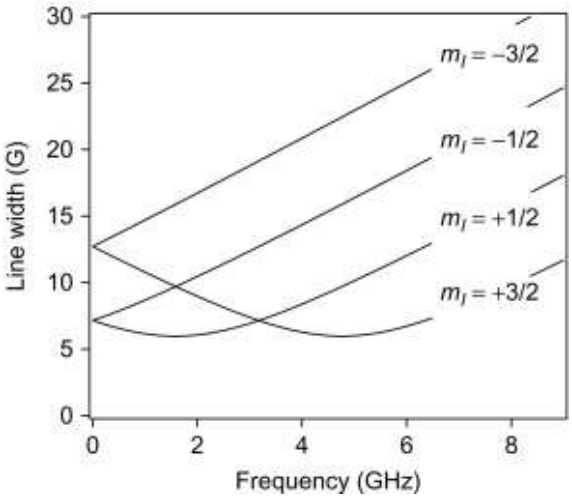

Figure 3. Frequency dependence of strain-dependent line widths in Cu(II) EPR.

Methods in Enzymology, Vol 563 (2015): pg. 341-361. DOI.

A second phenomenon of specific significance to copper is isotope broadening. Naturally abundant copper consists of ≈ 69% ^{63}Cu with g_n = 1.484 and Q/e = − 220 b (1b = 10^{-28} m^2), and ≈ 31% ^{65}Cu with g_n = 1.588 and Q/e = − 204b. There are three consequences of this isotopic distribution. The quadrupole moment ratio is ≈ 1.08, and the magnitude of the quadrupolar coupling itself is generally ≤ 15 MHz, i.e., ≤ 5 G, so any broadening due to the distinct quadrupole moments of ^{63}Cu and ^{65}Cu is limited to < 0.5 G and the isotopic dependence can usually be neglected. Similarly, while the field-(and frequency-)dependent nuclear Zeeman interaction is significant for Cu(II), ≈ 2 G at X-band, the difference in value between the two isotopes is only ≈ 0.14 G at X-band and, again, this difference can be neglected for X-band and lower frequencies in almost all cases. In contrast, the nuclear magnetic moment ratio of ≈ 0.93 is significant, as it applies to much larger absolute values. For a typical $A_{||}$(^{63}Cu) of 185 G, the corresponding value for $A_{||}$(^{65}Cu) is 198 G, i.e., $\Delta A_{||}$(^{65}Cu − ^{63}Cu) ≅ 13 G. A typical ^{14}N superhyperfine coupling is also ≈ 13 G. The relative displacements of the m_I = + 3/2, + 1/2, − 1/2, and − 1/2 manifolds due to ^{65}Cu from those due to ^{63}Cu are − 19.5, − 6,5, + 6.5, and + 19.5 G. Consequently, for each $A_{||}$(Cu) manifold, the ^{14}N superhyperfine patterns will experience "destructive interference," with the broadening of the outer lines of these patterns being particularly severe as the more intense of the ^{65}Cu lines are out of phase with the less intense of the ^{63}Cu lines and the natural isotopic abundance ensures almost complete cancellation. The intensities of the superhyperfine lines for the inner ± 1/2 patterns will no longer obey the symmetrical binomial distribution and a shoulder on the outer line will be expected due to the higher g_n, lower isotopic fraction ^{65}Cu contribution. The outer ± 3/2 patterns will be more distorted, with an isolated "extra" ^{65}Cu line outside the dominant ^{63}Cu pattern. In practice, the expected loss of resolution, particularly on the lower-field (outer) side of the resolved + 1/2 pattern, is indeed observed at frequencies where superhyperfine structure is resolved from samples containing naturally abundant isotopes of copper (Fig. 4). The effect of the isotopic constitution of naturally abundant copper on the observed perpendicular copper hyperfine splitting is much smaller than for the parallel splitting. $A_{\perp}$(Cu) values actually exhibit some rhombicity ($A_x \neq A_y$) and vary much more than the essentially isotropic but roughly similar values for coordinated nitrogen superhyperfine, with

Methods in Enzymology, Vol 563 (2015): pg. 341-361. DOI.

values of $A_{x/y}$(Cu) from 5 to 20 × 10^{-4} cm^{-1} reported (Ammeter et al., 1972, Hyde et al., 2013, Hyde et al., 2009 and Kowalski and Bennett, 2011). Taking an arbitrary value of 15 G for $A_{\perp}(^{63}Cu)$, then the value of $A_{\perp}(^{65}Cu)$ is expected to be ≈ 16.1 G; the resulting broadening of ≈ 1 G is tolerable (Hyde et al., 2013).

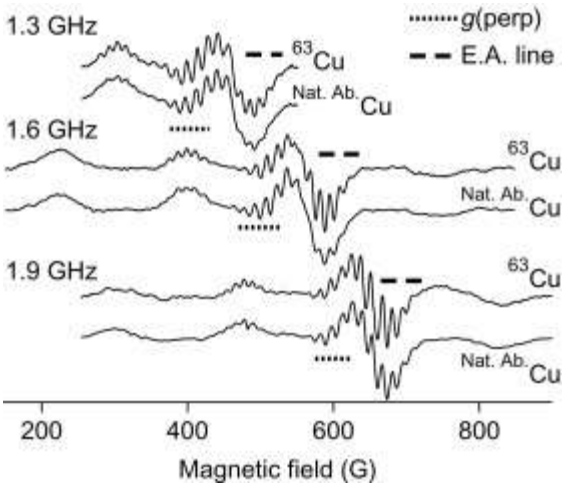

Figure 4. Low-frequency EPR of ^{63}Cu(II) and naturally abundant Cu(II). The dotted lines highlight the $g_{\perp}$ regions of the spectra and the dashed lines highlight the "extra absorption" or "overshoot" regions.

Finally, any discussion of EPR of Cu(II) would be incomplete without a discussion of the "overshoot" or "angular anomaly" that is a feature of Cu(II) EPR spectra (Ovchinnikov & Konstaninov, 1978). The overshoot line arises from the differential change in resonant field due to the orientation-dependent changes in the anisotropic **g** and **A**(Cu) tensors; phenomenologically, the hyperfine pattern expands "faster" than the *g*-value decreases, as the molecular orientation transitions from $x||\mathbf{B}$ or $y||\mathbf{B}$ to $z||\mathbf{B}$, as sketched in Fig. 5. At X-band (Fig. 5, top), the highest resonant field "overshoots" that corresponding to the highest-field hyperfine resonance of either of the principal electronic Zeeman resonances (hence the name) and manifests itself as an additional resonance in the powder spectrum that is easily mistaken for evidence of a rhombic **g** tensor with three distinct principal values (see Fig. 1, top). At lower frequencies, either one or two overshoot lines may appear within the field envelope of the spectrum (see Fig. 5, bottom), whereas simulations (Fig. 6) indicate that the overshoot line contributes to the highest field resonance in spectra recorded at frequencies up to 95 GHz (*g*-strain usually precludes clear experimental demonstration of this effect at frequencies beyond X-

band, though it has been demonstrated at 35 GHz) (Bennett & Hill, 2011). The primary consequences of the overlap of the overshoot line and the $g_{\perp}$ resonance are an inability to reliably count the number of lines in the patterns due to magnetic copper and nitrogen nuclei, and difficulty in extraction of spin-Hamiltonian parameters even by computer simulation, particularly where noncoincidence of **g** and **A** is significant. The combination of strain-broadening of the parallel resonances and the overlap of the overshoot line with the perpendicular resonances render X-band a frequency that is particularly unsuited for the high-resolution study of Cu(II)! It is with some sense of irony, then, that the reader may care to reflect on the fact that the overwhelming majority of EPR of Cu(II) is recorded at X-band, as evidenced by the observation that, of the 70 experimental EPR spectra reproduced in the Solomon review, 68 were recorded at X-band (the remaining two were at Q-band, 35 GHz) (Solomon et al., 2014).

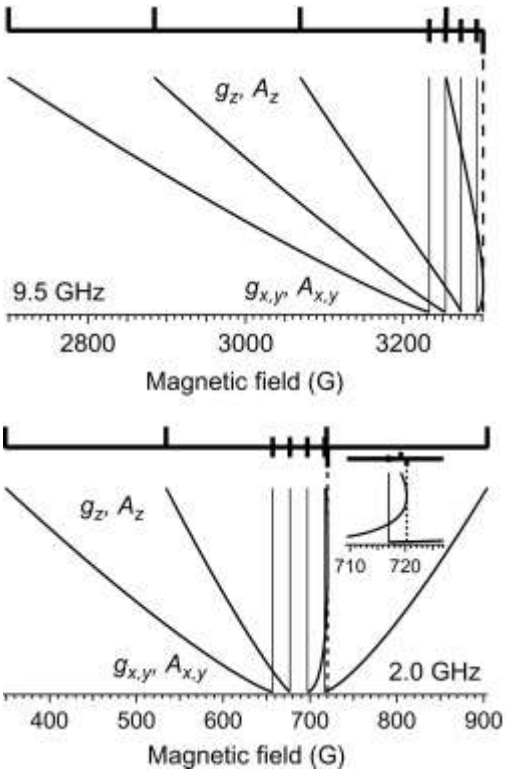

Figure 5. Schematic of the origin of the "extra absorption" or "overshoot" line at X- (top) and L- (bottom) bands.

Methods in Enzymology, Vol 563 (2015): pg. 341-361. DOI.

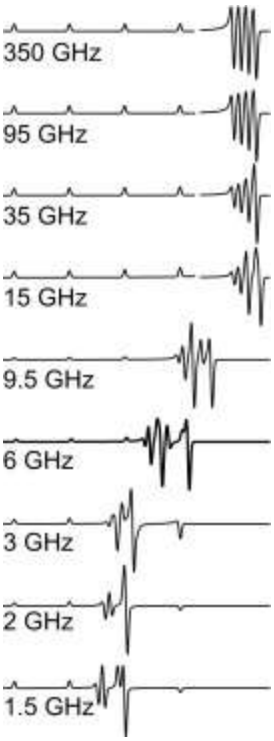

Figure 6. Frequency dependence of the effect of the overshoot line on the EPR spectra of Cu(II) from 1.5 to 350 GHz.

4. Low-Frequency EPR of Cu(II)

Multifrequency EPR, particularly EPR at < 9.5 GHz, has long been employed to better characterize the (equatorial) ligand coordination of Cu(II) (Antholine et al., 1992, Aronoff-Spencer et al., 2000, Burns et al., 2002, Burns et al., 2003, Chattopadhyay et al., 2005, Kroneck et al., 1988, Neese et al., 1996 and Rakhit et al., 1985) and the rationale for a truly multifrequency approach to EPR of Cu(II) is presented in the ABH review, in the wider context of multifrequency EPR in general (Antholine et al., 2011). The genesis of the rational application of low-frequency EPR to Cu(II) is to be found in the treatment of strains by Froncisz and Hyde (Froncisz et al., 1979, Froncisz and Hyde, 1980 and Hyde and Froncisz, 1982). This analysis and its experimental verification showed that in the region 1–4 GHz, one of the two lower-field parallel resonances is optimally resolved due to strain narrowing. The contemporaneous development of the loop-gap resonator (LGR) was also crucial to the adoption of low-frequency EPR for the high-resolution EPR study of Cu(II) (Froncisz and Hyde, 1982 and Hyde and Froncisz, 1986). The size of traditional cavity

Methods in Enzymology, Vol 563 (2015): pg. 341-361. DOI.

resonators for EPR scale essentially as the wavelength of the microwave radiation, λ, so the volume scales as the cube of λ, making the active volume of a 2 GHz resonator some 75 × larger than a traditional X-band cavity, and requiring some 20 mL of sample, prohibitive for many biological systems. The development of the LGR facilitated the use of much smaller samples, and fuelled the highly productive application of S-band (3.4 GHz) EPR to biological and inorganic copper systems by Antholine et al. (2011). More recently, Hyde, Sidabras, and coworkers developed, first, a one-loop-one-gap 0.5 mL LGR for EPR at 1.9 GHz (Hyde et al., 2009), and subsequently, a 0.25 mL two-loop-one-gap resonator with improved microwave shielding and superior mechanical and temperature stability (Hyde et al., 2013 and Kowalski and Bennett, 2011). These structures allowed for the study of limited biological samples such as PrP and are shown along with the corresponding cavity resonator in Fig. 7.

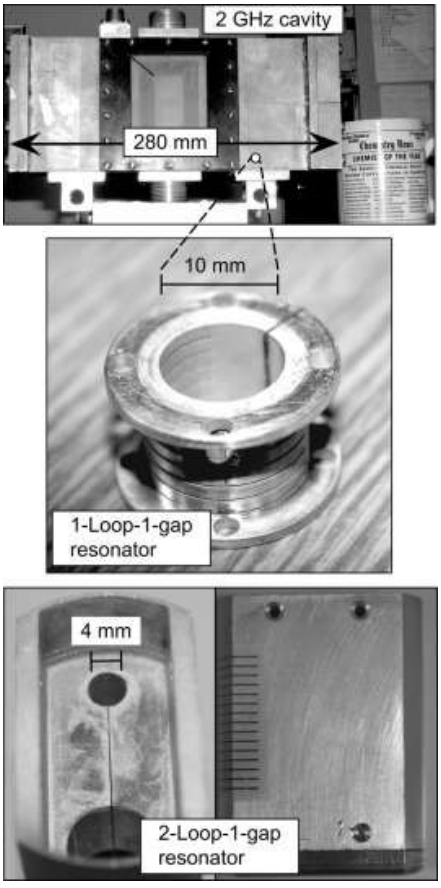

Figure 7. Resonant microwave structures at L-band. Top, resonant cavity. Middle, 1-loop-1-gap 0.5 mL loop-gap resonator. Bottom, 2-loop-1-gap 0.25 mL loop-gap resonator.

Methods in Enzymology, Vol 563 (2015): pg. 341-361. DOI.

Another development that spurred the adoption of low-frequency EPR was improved, user-friendly computer simulations (Hanson et al., 2004 and Hanson et al., 2003). Indeed, the adoption of 2 GHz as the frequency of choice for the study of Cu(II) was based upon computer simulations of the EPR absorption envelope (Fig. 8). As is clear from the figure, as the microwave frequency is lowered from X-band (9.5 GHz), an overshoot line emerges from the complex high-field region of the higher frequency spectra, until it is optimally resolved from other spectra features at 2 GHz. At yet lower frequencies, the energy levels between which the EPR transitions occur become complex themselves (Fig. 9) and the spectra at 1 GHz reflect this complexity. At 2 GHz, though, the overshoot line is highly resolved and can now be viewed as a source of information, rather than a complicating feature. The "anatomy" of a typical L-band spectrum at 1.85 GHz is illustrated in Fig. 10. Here, three of the hyperfine manifolds of the parallel electronic Zeeman resonance are resolved, PA, PB, & PD, with ^{14}N superhyperfine structure observed on the PB (m_I = + 1/2) line with $A_{||}(4 \times {}^{14}\mathrm{N})$ = 12.3 G (the superhyperfine lines are labeled PB1 to PB7 in the lower tile of the figure). The EPR absorption manifolds are shown below the spectrum, calculated without the ^{14}N superhyperfine contribution. The central "perpendicular" region of the spectrum is composed of two regions. One exhibits superhyperfine structure with a splitting equal to the value $A_{\perp}(^{14}\mathrm{N})$ = 14.4 G (labeled A1–A6). This region corresponds to the genuine perpendicular electronic Zeeman resonance, $g_{\perp}$. The adjacent region (B1–B6) exhibits a splitting of 13.1 G, intermediate between the values for $A_{||}$ and $A_{\perp}$, and corresponds to the overshoot line of indeterminate orientation (it can, in fact, be estimated by "roadmap" simulations). The center of the pattern due to the overshoot line can be determined from the EPR absorption spectrum, where it dominates the overlapping but much less intense perpendicular feature of the $m_I = -3/2$ manifold, and analysis (usually by simulation) of the high-field side of this feature provides the number of equatorially coordinated nitrogen atoms. This method was successfully used to determine the coordination of copper bound to a PrP fragment that had defied characterization by X- and S-band EPR, and ESEEM spectroscopy (Chattopadhyay et al., 2005 and Hyde et al., 2009). The characterization of other prion-bound species of copper was subsequently and similarly carried out, with additional

Methods in Enzymology, Vol 563 (2015): pg. 341-361. DOI.

verification of the number of coordinated nitrogen atoms being provided by analyses of the parities of the Fourier transforms of the EPR spectra (Della Lunga et al., 1995, Kowalski and Bennett, 2011 and Pasenkiewicz-Gierula, et al., 1987). This latter, often neglected, method discriminates between odd and even numbers of magnetic nuclei that contribute essentially equally to a superhyperfine pattern, and is particularly useful for discriminating 3 versus 4 coordinated nitrogens where the data quality does not allow definitive identification of the weakest outer superhyperfine line.

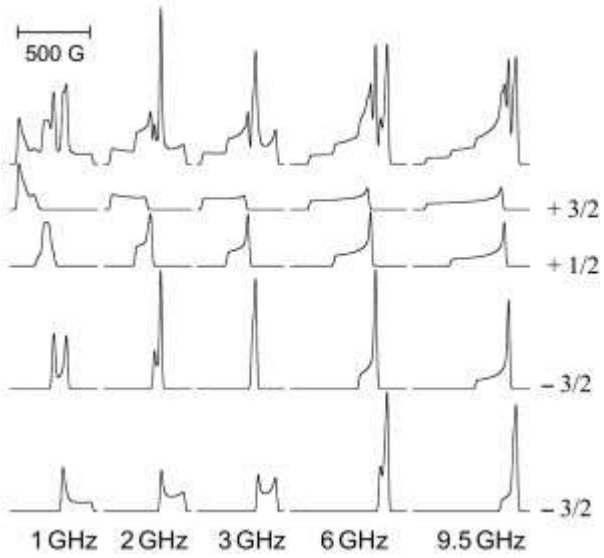

Figure 8. Calculated absorption spectra of Cu(II) and their hyperfine manifolds at various frequencies.

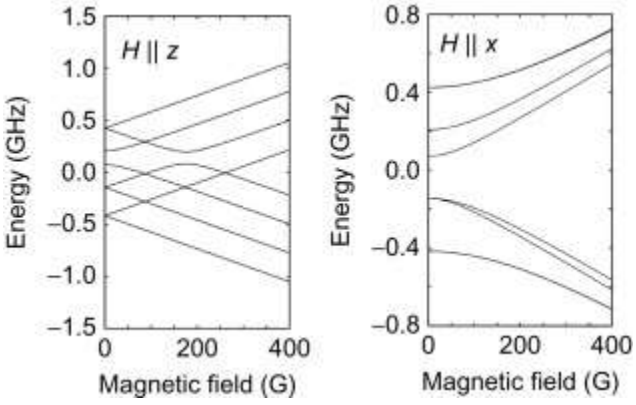

Figure 9. Energy levels of Cu(II) at low resonant magnetic fields.

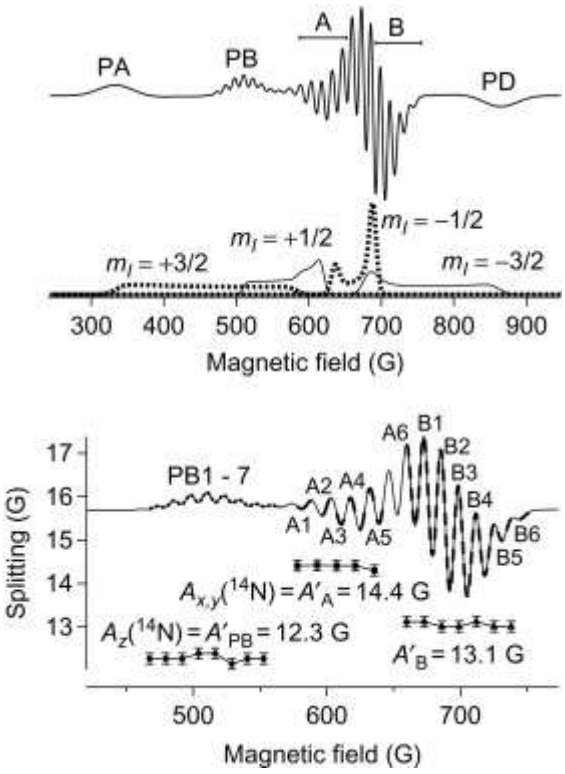

Figure 10. The anatomy of a typical L-band EPR spectrum of nitrogen-coordinated Cu(II).

5. Nonadiabatic Rapid Sweep (NARS) EPR Spectroscopy

NARS is a term used to describe a rapid scanning methodology in which the magnetic field is scanned sufficiently rapidly through the spectrum to significantly abate 1/*f* noise but sufficiently slowly so as to maintain the system in thermal equilibrium (Kittell et al., 2011). Phase-sensitive detection is dispensed with and the spectral display is that of a pure absorption spectrum with about 4 × the signal-to-noise ratio of conventional EPR under otherwise equivalent conditions with no attendant modulation broadening or distortion. The technique was developed for the purpose of detecting small line-broadening due to dipolar coupling between two spin labels separated by up to 40 Å, and low frequency (1–2 GHz) was employed in order to collapse the **g** tensor at the low resonant fields and, hence, increase the distance limit of the method (Kittell et al., 2012). The enhanced signal to noise, the flexibility of multiple data processing options on the same dataset, the absence of field modulation artifacts, and the development at L-

band were seen as attractive for the study of Cu(II), and NARS was subsequently adapted for that purpose by the present authors and coworkers (Hyde et al., 2013). The major adaptation arose because the field envelope of the Cu(II) spectrum is far too wide to be scanned at audio frequencies using conventional electromagnetic coils. The solution was to scan the spectrum in segments and concatenate the fragments (shown schematically in Fig. 11). The fragment size was deliberately chosen so as not to correspond to the expected width or separation of any features in the spectrum. Artifacts that occurred during the automated concatenation of the fragments were then isolated in the Fourier transform and edited prior to reverse transformation back to the absorption spectrum. This proved to be highly effective. The goal was to use the NARS method to characterize nitrogen coordinated to copper. However, the absorption display was not ideal for displaying the superhyperfine pattern due to the intense underlying body of the absorption spectrum, and various methods of transforming the dataset to a derivative-like display were evaluated. The most successful one appeared to be a simple moving difference (MDIFF) algorithm, that had not apparently been employed previously in the context of EPR spectroscopy, but that was an effective way of preferentially increasing the intensity of narrow features relative to broad ones (Hyde et al., 2013). The MDIFF algorithm can equally well be applied to experimental and simulated absorption data, facilitating the use of simulations for spectral analysis. Further, the MDIFF amplitude (analogous to the field modulation amplitude) can be arbitrarily varied, and the amplitude at which the spectral lines begin to lose intensity through broadening provided a sensitive and reproducible method for determining line widths. Finally, it was found that the MDIFF algorithm was an effective and selective low-frequency filter, much more so than mere averaging, that was ideally suited to EPR spectra that contain narrow features and that require stringent conditions for high-resolution, but that overlap broad, gross features with wide field envelopes. The technique is thus eminently suited to low-frequency EPR of copper, though many other applications can be imagined.

Methods in Enzymology, Vol 563 (2015): pg. 341-361. DOI.

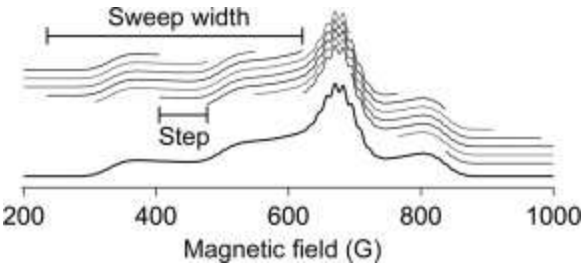

Figure 11. Schematic of the collection of NARS EPR data on Cu(II). In practice, the sweep widths are much smaller than shown here, e.g., 5 G.

References

Abrakhmanov and Ivanova, 1978. R.S. Abrakhmanov, T.A. Ivanova. Possible use of low-frequency ESR to estimate the quadrupole coupling constant in copper(II) complexes. *Journal of Structural Chemistry*, 19 (1978), pp. 145–148

Ammeter et al., 1972. J. Ammeter, G.H. Rist, H.A. Günthard. Influence of the host lattice upon EPR coupling parameters and d-d transitions of planar copper (II) complexes. *The Journal of Chemical Physics*, 57 (1972), pp. 3852–3866

Antholine et al., 2011. W.E. Antholine, B. Bennett, G.R. Hanson. Copper coordination environments. S.K. Misra (Ed.), *Multifrequency electron paramagnetic resonance*, Wiley-VCH, Berlin (2011), pp. 647–715

Antholine et al., 1992. W.E. Antholine, D.H.W. Kastrau, G.C.M. Steffens, G. Buse, W.G. Zumft, P.M.H. Kroneck. A comparative EPR investigation of the multicopper proteins nitrous oxide reductase and cytochrome c oxidase. *European Journal of Biochemistry*, 209 (1992), pp. 875–881

Arnesano et al., 2009. F. Arnesano, S. Scintilla, V. Calò, E. Bonfrate, C. Ingrosso, M. Losacco, *et al.* Copper-triggered aggregation of ubiquitin. *PLoS One*, 4 (2009), p. e7052

Aronoff-Spencer et al., 2000. E. Aronoff-Spencer, C.S. Burns, N.I. Avdievich, G.J. Gerfen, J. Peisach, W.E. Antholine, *et al.* Identification of the Cu2 + binding sites in the N-terminal domain of the prion protein by EPR and CD spectroscopy. *Biochemistry*, 39 (45) (2000), pp. 13760–13771

Barnham and Bush, 2008. K.J. Barnham, A.I. Bush. Metals in Alzheimer's and Parkinson's diseases. *Current Opinion in Chemical Biology*, 12 (2) (2008), pp. 222–228

Bayer et al., 2006. T.A. Bayer, S. Schafer, H. Breyhan, O. Wirths, C. Treiber, G. Multhaup. A vicious circle: Role of oxidative stress, intraneuronal abeta and Cu in Alzheimer's disease. *Clinical Neuropathology*, 25 (4) (2006), pp. 163–171

Belford and Duan, 1978. R.L. Belford, D.C. Duan. Determination of nuclear quadrupolar coupling by simulation of EPR spectra of frozen solutions. *Journal of Magnetic Resonance*, 29 (1978), pp. 293–307

Bennett and Hill, 2011. B. Bennett, B.C. Hill. Avoiding premature oxidation during the binding of Cu(II) to a dithiolate site in BsSCO. A rapid freeze-quench EPR study. *FEBS Letters*, 585 (6) (2011), pp. 861–864

Brown, 2009. D.R. Brown. Metal binding to alpha-synuclein peptides and its contribution to toxicity. *Biochemical and Biophysical Research Communications*, 380 (2009), pp. 377–381

Burns et al., 2002. C.S. Burns, E. Aronoff-Spencer, C.M. Dunham, P. Lario, N.I. Avdievich, W.E. Antholine, *et al.* Molecular features of the copper binding sites in the octarepeat domain of the prion protein. *Biochemistry*, 41 (12) (2002), pp. 3991–4001

Burns et al., 2003. C.S. Burns, E. Aronoff-Spencer, G. Legname, S.B. Prusiner, W.E. Antholine, G.J. Gerfen, *et al.* Copper coordination in the full-length, recombinant prion protein. *Biochemistry*, 42 (22) (2003), pp. 6794–6803

Bush, 2008. A.I. Bush. Drug development based on the metals hypothesis of Alzheimer's disease. *Journal of Alzheimer's Disease*, 15 (2) (2008), pp. 223–240

Bush and Tanzi, 2008. A.I. Bush, R.E. Tanzi. Therapeutics for Alzheimer's disease based on the metal hypothesis. *Neurotherapeutics*, 5 (3) (2008), pp. 421–432

Chattopadhyay et al., 2005. M. Chattopadhyay, E.D. Walter, D.J. Newell, P.J. Jackson, E. Aronoff-Spencer, J. Peisach, *et al.* The octarepeat domain of the prion protein binds Cu(II) with three distinct coordination modes at pH 7.4. *Journal of the American Chemical Society*, 127 (2005), pp. 12647–12656

Comba et al., 2008. P. Comba, L.R. Gahan, G. Haberhauer, G.R. Hanson, C.J. Noble, B. Seibold, *et al.* Copper(II) coordination chemistry of westiellamide and its imidazole, oxazole, and thiazole analogues. *Chemistry—A European Journal*, 14 (2008), pp. 4394–4403

Crouch et al., 2009. P.J. Crouch, L.W. Hung, P.A. Adlard, M. Cortes, V. Lal, G. Filiz, *et al.* Increasing Cu bioavailability inhibits Abeta oligomers and tau phosphorylation. *Proceedings of the National Academy of Sciences of the United States of America*, 106 (2) (2009), pp. 381–386

Crouch et al., 2007. P.J. Crouch, A.R. White, A.I. Bush. The modulation of metal bio-availability as a therapeutic strategy for the treatment of Alzheimer's disease. *The FEBS Journal*, 274 (15) (2007), pp. 3775–3783

de Bie et al., 2007. P. de Bie, P. Muller, C. Wijmenga, L.W. Klomp. Molecular pathogenesis of Wilson and Menkes disease: Correlation of mutations

with molecular defects and disease phenotypes. *Journal of Medical Genetics*, 44 (2007), pp. 673–688

Della Lunga et al., 1995. G. Della Lunga, R. Pogni, R. Basosi. Discrimination of copper-nitrogen ligand coordination by Fourier analysis of EPR spectra in mobile phase. *Journal of Magnetic Resonance, Series A*, 114 (1995), pp. 174–178

Drew et al., 2009. S.C. Drew, C.J. Noble, G.R. Hanson, C.L. Masters, K.J. Barnham. Pleomorphic Cu2 + coordination of Alzheimer's amyloid-*β* peptide. *Journal of the American Chemical Society*, 131 (2009), pp. 1195–1207

Froncisz and Hyde, 1980. W. Froncisz, J.S. Hyde. Broadening by strains of lines in the g-parallel region of Cu2 + EPR spectra. *The Journal of Chemical Physics*, 73 (1980), pp. 3123–3131

Froncisz and Hyde, 1982. W. Froncisz, J.S. Hyde. The loop-gap resonator: A new microwave lumped circuit ESR sample structure. *Journal of Magnetic Resonance*, 47 (1982), pp. 515–521

Froncisz et al., 1980. W. Froncisz, T. Sarna, J.S. Hyde. Cu2 + probe of metal-ion binding sites in melanin using electron paramagnetic resonance spectroscopy. I. Synthetic melanins. *Archives of Biochemistry and Biophysics*, 202 (1) (1980), pp. 289–303

Froncisz et al., 1979. W. Froncisz, C.P. Scholes, J.S. Hyde, Y.H. Wei, T.E. King, R.W. Shaw, *et al.* Hyperfine structure resolved by 2 to 4 GHz EPR of cytochrome c oxidase. *The Journal of Biological Chemistry*, 254 (16) (1979), pp. 7482–7484

Furukawa et al., 2008. T. Furukawa, M. Komatsu, R. Ikeda, K. Tsujikawa, S. Akiyama. Copper transport systems are involved in multidrug resistance and drug transport. *Current Medicinal Chemistry*, 15 (2008), pp. 3266–3278

Hanson et al., 2004. G.R. Hanson, K.E. Gates, C.J. Noble, M. Griffin, A. Mitchell, S. Benson. XSophe-sophe-XeprView: A computer simulation suite (v.1.1.3) for the analysis of continuous wave EPR spectra. *Journal of Inorganic Biochemistry*, 98 (2004), pp. 903–916

Hanson et al., 2003. G.R. Hanson, K.E. Gates, C.J. Noble, A. Mitchell, S. Benson, M. Griffin, *et al.* XSophe-sophe-XeprView: A computer simulation software suite for the analysis of continuous wave EPR spectra. M. Shiotani, A. Lund (Eds.), *EPR of free radicals in solids: Trends in methods and applications*, Kluwer Press, Dordrecht (2003), pp. 197–237

Huang et al., 1999. X. Huang, M.P. Cuajungco, C.S. Atwood, M.A. Hartshorn, J.D. Tyndall, G.R. Hanson, *et al.* Cu(II) potentiation of Alzheimer abeta neurotoxicity. Correlation with cell-free hydrogen peroxide production and metal reduction. *The Journal of Biological Chemistry*, 274 (52) (1999), pp. 37111–37116

Hyde et al., 1986. J.S. Hyde, W.E. Antholine, W. Froncisz, R. Basosi. EPR determination of the number of nitrogens coordinated to Cu in square-planar complexes. N. Nicolai, G. Valensin (Eds.), *Advanced magnetic resonance techniques in systems of high molecular complexity*, Birkhauser, Boston (1986), pp. 363–384

Hyde et al., 2013. J.S. Hyde, B. Bennett, A.W. Kittell, J.M. Kowalski, J.W. Sidabras. Moving difference (MDIFF) non-adiabatic rapid sweep (NARS) EPR of copper(II). *Journal of Magnetic Resonance*, 236 (2013), pp. 15–25

Hyde et al., 2009. J.S. Hyde, B. Bennett, E.D. Walter, G.L. Millhauser, G.W. Sidabras, W.E. Antholine. EPR of Cu prion protein constructs at 2.0 GHz using the g-perpendicular region to characterize nitrogen ligation. *Biophysical Journal*, 96 (2009), pp. 3354–3362

Hyde and Froncisz, 1982. J.S. Hyde, W. Froncisz. The role of microwave frequency in EPR spectroscopy of copper complexes. *Annual Review of Biophysics and Bioengineering*, 11 (1982), pp. 391–417

Hyde and Froncisz, 1986. J.S. Hyde, W. Froncisz. Loop gap resonators. *Specialist Periodical Reports of the Royal Society of Chemistry*, 10 (1986), pp. 175–184

Kittell et al., 2011. A.W. Kittell, T.G. Camenisch, J.J. Ratke, J.W. Sidabras, J.S. Hyde. Detection of undistorted continuous wave (CW) electron paramagnetic resonance (EPR) spectra with non-adiabatic rapid sweep (NARS) of the magnetic field. *Journal of Magnetic Resonance*, 211 (2011), pp. 228–233

Kittell et al., 2012. A.W. Kittell, E.J. Hustedt, J.S. Hyde. Inter-spin distance determination using L-band (1–2 GHz) non-adiabatic rapid sweep electron paramagnetic resonance (NARS EPR). *Journal of Magnetic Resonance*, 221 (2012), pp. 51–56

Kittell and Hyde, 2015. A.W. Kittell, J.S. Hyde. Spin-label CW microwave power saturation and rapid passage with triangular non-adiabatic rapid sweep (NARS) and adiabatic rapid passage (ARP) EPR spectroscopy. *Journal of Magnetic Resonance*, 255 (2015), pp. 68–76

Kochelaev and Yablokov, 1995. B.I. Kochelaev, Y.V. Yablokov. *The beginning of paramagnetic resonance.* World Scientific, Singapore (1995)

Kowalski and Bennett, 2011. J.M. Kowalski, B. Bennett. Spin Hamiltonian parameters for Cu(II)-prion peptide complexes from L-band electron paramagnetic resonance spectroscopy. *Journal of the American Chemical Society*, 133 (2011), pp. 1814–1823

Kroneck et al., 1988. P.M.H. Kroneck, W.A. Antholine, J. Riester, W.G. Zumft. The cupric site in nitrous oxide reductase contains a mixed-valence [Cu(II), Cu(I)] binuclear center: A multi-frequency electron paramagnetic resonance investigation. *FEBS Letters*, 242 (1988), pp. 70–74

Kuo et al., 2007. M.T. Kuo, H.H. Chen, I.S. Song, N. Savaraj, T. Ishikawa. The roles of copper transporters in cisplatin resistance. *Cancer Metastasis Reviews*, 26 (2007), pp. 71–83

La Fontaine and Mercer, 2007. S. La Fontaine, J.F. Mercer. Trafficking of the copper-ATPases, ATP7A and ATP7B: Role in copper homeostasis. *Archives of Biochemistry and Biophysics*, 463 (2007), pp. 149–167

Leach et al., 2006. S.P. Leach, M.D. Salman, D. Hamar. Trace elements and prion diseases: A review of the interactions of copper, manganese and zinc with the prion protein. *Animal Health Research Reviews*, 7 (1–2) (2006), pp. 97–105

Linder and Hazegh-Azam, 1996. M.C. Linder, M. Hazegh-Azam. Copper biochemistry and molecular biology. *The American Journal of Clinical Nutrition*, 63 (1996), pp. 797S–811S

Malmstrøm and Leckner, 1998. B.G. Malmstrøm, J. Leckner. The chemical biology of copper. *Current Opinion in Chemical Biology*, 2 (1998), pp. 286–292

Maynard et al., 2005. C.J. Maynard, A.I. Bush, C.L. Masters, R. Cappai, Q.X. Li. Metals and amyloid-beta in Alzheimer's disease. *International Journal of Experimental Pathology*, 86 (3) (2005), pp. 147–159

Millhauser, 2007. G.L. Millhauser. Copper and the prion protein: Methods, structures, function, and disease. *Annual Review of Physical Chemistry*, 58 (2007), pp. 299–320

Nadal et al., 2007. R.C. Nadal, S.R. Abdelraheim, M.W. Brazier, S.E. Rigby, D.R. Brown, J.H. Viles. Prion protein does not redox-silence Cu2 +, but is a sacrificial quencher of hydroxyl radicals. *Free Radical Biology & Medicine*, 42 (1) (2007), pp. 79–89

Neese et al., 1996. F. Neese, W.G. Zumft, W.E. Antholine, P.M.H. Kroneck. The purple mixed valence CuA center in nitrous oxide reductase: EPR of the copper-63 and copper-65, and both copper-65 and [15N]Histidine-enriched enzyme and a molecular orbital interpretation. *Journal of the American Chemical Society*, 118 (1996), pp. 8692–8699

Ovchinnikov and Konstaninov, 1978. I.V. Ovchinnikov, V.N. Konstaninov. Extra absorption peaks in EPR spectra of systems with anisotropic g-tensor and hyperfine structure in powders and glasses. *Journal of Magnetic Resonance*, 32 (1978), pp. 179–190

Park et al., 2010. K.H. Park, D.G. Shin, J.R. Kim, J.H. Hong, K.H. Cho. The functional and compositional properties of lipoproteins are altered in patients with metabolic syndrome with increased cholesteryl ester transfer protein activity. *International Journal of Molecular Medicine*, 25 (2010), pp. 129–136

Pasenkiewicz-Gierula, Antholine, et al., 1987. M. Pasenkiewicz-Gierula, W.E. Antholine, W.K. Subczynski, O. Baffa, J.S. Hyde, D.H. Petering.

Assessment of the ESR spectra of CuKTSM2. *Inorganic Chemistry*, 26 (1987), pp. 3945–3949

Pasenkiewicz-Gierula, et al., 1987. M. Pasenkiewicz-Gierula, W. Froncisz, R. Basosi, W.E. Antholine, J.S. Hyde. Multifrequency ESR with Fourier analysis of CuII(His)$_n$ (His = histidine). 2. Mobile phase. *Inorganic Chemistry*, 26 (1987), pp. 801–805

Peisach and Blumberg, 1974. J. Peisach, W.E. Blumberg. Structural implications derived from the analysis of electron paramagnetic resonance spectra of natural and artificial copper proteins. *Archives of Biochemistry and Biophysics*, 165 (1974), pp. 691–708

Perrone et al., 2009. L. Perrone, E. Mothes, M. Vignes, A. Mockel, C. Figueroa, M.C. Miquel, *et al.* Copper transfer from Cu-Abeta to human serum albumin inhibits aggregation, radical production and reduces Abeta toxicity. *Chembiochem*, 11 (2009), pp. 110–118

Pfeiffer, 2007. R.F. Pfeiffer. Wilson's disease. *Seminars in Neurology*, 27 (2007), pp. 123–132

Pilbrow, 1990. J.R. Pilbrow. *Transition ion electron paramagnetic resonance.* Oxford University Press, Oxford (1990)

Puig and Thiele, 2002. S. Puig, D.J. Thiele. Molecular mechanisms of copper uptake and distribution. *Current Opinion in Chemical Biology*, 6 (2002), pp. 171–180

Rakhit et al., 1985. G. Rakhit, W.E. Antholine, W. Froncisz, J.S. Hyde, J.R. Pilbrow, G.R. Sinclair, *et al.* Direct evidence of nitrogen coupling in the copper(II) complex of bovine serum albumin by S-band electron spin resonance technique. *Journal of Inorganic Biochemistry*, 25 (3) (1985), pp. 217–224

Roucou and LeBlanc, 2005. X. Roucou, A.C. LeBlanc. Cellular prion protein neuroprotective function: Implications in prion diseases. *Journal of Molecular Medicine*, 83 (2005), pp. 3–11

Solomon et al., 2014. E.I. Solomon, D.E. Heppner, E.M. Johnston, J.W. Ginsbach, J. Cirera, M. Qayyum, *et al.* Copper active sites in biology. *Chemical Reviews*, 114 (7) (2014), pp. 3659–3853

Tisato et al., 2009. F. Tisato, C. Marzano, M. Porchia, M. Pellei, C. Santini. Copper in diseases and treatments, and copper-based anticancer strategies. *Anti-Cancer Agents in Medicinal Chemistry*, 9 (2009), pp. 185–211

Valentine and Gralla, 2002. J.S. Valentine, E.B. Gralla. Copper-containing molecules. *Advances in protein chemistry*, Academic Press, New York (2002)

Varela-Nallar et al., 2006. L. Varela-Nallar, A. Gonzalez, N.C. Inestrosa. Role of copper in prion diseases: Deleterious or beneficial? *Current Pharmaceutical Design*, 12 (20) (2006), pp. 2587–2595

Varela-Nallar, et al., 2006. L. Varela-Nallar, E.M. Toledo, M.A. Chacon, N.C. Inestrosa. The functional links between prion protein and copper. *Biological Research*, 39 (1) (2006), pp. 39–44

Vucic and Kiernan, 2009. S. Vucic, M.C. Kiernan. Pathophysiology of neurodegeneration in familial amyotrophic lateral sclerosis. *Current Molecular Medicine*, 9 (2009), pp. 255–272

Wang and Colon, 2007 L. Wang, W. Colon. Effect of zinc, copper, and calcium on the structure and stability of serum amyloid A. *Biochemistry*, 46 (2007), pp. 5562–5569

White and Belford, 1976. L.K. White, R.L. Belford. Quadrupole coupling constants of square-planar copper(II)-sulfur complexes from single-crystal electron paramagnetic resonance spectroscopy. *Journal of the American Chemical Society*, 98 (1976), pp. 4428–4438

Wong et al., 2004. E. Wong, A.M. Thackray, R. Bujdoso. Copper induces increased beta-sheet content in the scrapie-susceptible ovine prion protein PrPVRQ compared with the resistant allelic variant PrPARR. *The Biochemical Journal*, 380 (Pt 1) (2004), pp. 273–282

Wright and Brown, 2008. J.A. Wright, D.R. Brown. Alpha-synuclein and its role in metal binding: Relevance to Parkinson's disease. *Journal of Neuroscience Research*, 88 (2008), pp. 496–503

Zhang et al., 2009. Y. Zhang, M. Li, Q. Yao, C. Chen. Roles and mechanisms of copper transporting ATPases in cancer pathogenesis. *Medical Science Monitor*, 15 (2009), pp. RA1–RA5

Zidar et al., 2008. J. Zidar, E.T. Pirc, M. Hodoscek, P. Bukovec. Copper(II) ion binding to cellular prion protein. *Journal of Chemical Information and Modeling*, 48 (2) (2008), pp. 283–287

Methods in Enzymology, Vol 563 (2015): pg. 341-361. DOI.